AD-A094 254 ARNOLD ENGINEERING DEVELOPMENT CENTER ARNOLD AFS TN F/G 20/4
STING INTERFERENCE EFFECTS ON A 7 DEG CONE AS DETERMINED BY MEA--ETC(U)
DEC 79 F B CYRAN
UNCLASSIFIED AEDC-TSR-79-P75 NL

1 OF 1
AD A
094254

END
DATE
FILMED
2-81
DTIC

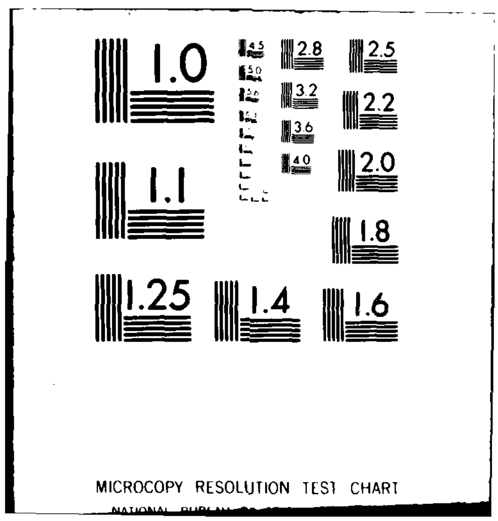
1.0
1.1
1.25
1.4
1.6
1.8
2.0
2.2
2.5
2.8
3.2
3.6
4.0
4.5
5.0
MICROCOPY RESOLUTION TEST CHART

AEDC-TSR-79-P75

LEVEL II

2

STING INTERFERENCE EFFECTS ON A 7 DEG CONE AS DETERMINED BY MEASUREMENTS OF DYNAMIC STABILITY DERIVATIVES AND BASE PRESSURE FOR MACH NUMBERS 0.2 THROUGH 1.3

F. B. Cyran

ARO, Inc.

AD A094254

December 1979

Final Report for Period September 26, 1979 to October 3, 1979

ARNOLD ENGINEERING DEVELOPMENT CENTER
ARNOLD AIR FORCE STATION, TENNESSEE
AIR FORCE SYSTEMS COMMAND
UNITED STATES AIR FORCE

81 1 27 022

NOTICES

APPROVAL STATEMENT

This report has been reviewed and approved.

Walter P. West

WALTER P. WEST, Capt, USAF
Test Director, PWT Division
Directorate of Test Operations

Approved for publication:

FOR THE COMMANDER

John C. Hartney

JOHN C. HARTNEY, Colonel, USAF
Director of Test Operations
Deputy for Operations

REPORT DOCUMENTATION PAGE		READ INSTRUCTIONS BEFORE COMPLETING FORM
1. REPORT NUMBER AEDC-TSR-79-P75	2. GOVT ACCESSION NO. AD-A094254	3. RECIPIENT'S CATALOG NUMBER
4. TITLE (and Subtitle) STING INTERFERENCE EFFECTS ON A 7 DEG CONE AS DETERMINED BY MEASUREMENTS OF DYNAMIC STABILITY DERIVATIVES AND BASE PRESSURE FOR MACH NUMBERS 0.2 THROUGH 1.3		5. TYPE OF REPORT & PERIOD COVERED Final Report, September 26, 1979 to October 3, 1979
		6. PERFORMING ORG. REPORT NUMBER
7. AUTHOR(s) F. B. Cyran, ARO, Inc., a Sverdrup Corporation Company		8. CONTRACT OR GRANT NUMBER(s)
9. PERFORMING ORGANIZATION NAME AND ADDRESS Arnold Engineering Development Center/DOT Air Force Systems Command Arnold Air Force Station, Tennessee 37389		10. PROGRAM ELEMENT, PROJECT, TASK AREA & WORK UNIT NUMBERS Program Element 65807F
11. CONTROLLING OFFICE NAME AND ADDRESS Arnold Engineering Development Center/DOS Air Force Systems Command Arnold Air Force Station, TN 37389		12. REPORT DATE December 1979
		13. NUMBER OF PAGES 38
14. MONITORING AGENCY NAME & ADDRESS (if different from Controlling Office)		15. SECURITY CLASS. (of this report) UNCLASSIFIED
		15a. DECLASSIFICATION/DOWNGRADING SCHEDULE N/A

16. DISTRIBUTION STATEMENT (of this Report)

Approved for public release; distribution unlimited.

17. DISTRIBUTION STATEMENT (of the abstract entered in Block 20, if different from Report)

18. SUPPLEMENTARY NOTES

Available in Defense Technical Information Center (DTIC).

19. KEY WORDS (Continue on reverse side if necessary and identify by block number)

dynamic stability	sting interference
pitch damping	splitter plates
yaw damping	yaw damping as a function of angle of attack
forced oscillation	
transonic flow	

20. ABSTRACT (Continue on reverse side if necessary and identify by block number)

The effects of sting support interference were investigated on the measurements of pitch damping, yaw damping, pitching moment slope, pitching moment and base pressure. The model was a 15 percent spherically blunt 7 deg cone. The forced oscillation technique was used to obtain data at Mach numbers 0.2 to 1.3 and Reynolds numbers, based on model base diameter, of 0.2 million to 3.6 million. The amplitude of oscillation was ±1 deg, and the reduced frequency parameter ranged from 0.006 to 0.049. The test was conducted at two oscillation frequencies, nominally 3.1 and 5.6 Hz. Pitch damping data were obtained

DD FORM 1 JAN 73 1473 EDITION OF 1 NOV 65 IS OBSOLETE

20. 3.4

at angles of attack of 0 to 28 deg, and yaw damping data were obtained at angles of attack of 0 to 20 deg. The effective sting length was varied from 1 to 1.4 model diameters. The interference effects of two types of model wake splitter plates were also investigated. The data obtained from this test at the transonic test conditions agreed with the results extrapolated from previous tests at AEDC at supersonic-hypersonic test conditions.

CONTENTS

		Page
	NOMENCLATURE	3
1.0	INTRODUCTION	5
2.0	APPARATUS	
	2.1 Test Facility	5
	2.2 Test Article	6
	2.3 Test Mechanism	6
	2.4 Test Instrumentation	
	2.4.1 Forced Oscillation Instrumentation	7
	2.4.2 Model Base Pressure Instrumentation	8
3.0	TEST DESCRIPTION	
	3.1 Test Conditions and Procedures	
	3.1.1 General	8
	3.1.2 Data Acquisition	9
	3.2 Data Reduction	9
	3.3 Uncertainty of Measurements	10
4.0	DATA PACKAGE PRESENTATION	11
	REFERENCES	11

APPENDIXES

I. ILLUSTRATIONS

Figure		
1.	Model Details	13
2.	Boundary Layer Trip Details	14
3.	Details of Model Support Configurations	
	a. Interference Sting, LS/D = 1.0	15
	b. Clean Sting, LS/D = 3.3	15
4.	Splitter Plate Details	
	a. Plate 1	16
	b. Plate 8	16
5.	Details of Splitter Plate Configurations	
	a. Plate 1 Installed, LS/D = 1.0	17
	b. Plate 8 Installed, LS/D = 3.3	17
6.	Photographs of Splitter Plate Installation	
	a. Plate 1 Installed, LS/D = 1.0	18
	b. Plate 8 Installed, LS/D = 3.3	18
7.	Model Installation Sketch in PWT Aerodynamic Wind Tunnel (4T)	19
8.	Photograph of Model Installation in PWT Aerodynamic Wind Tunnel (4T)	20
9.	Details of VKF 1.C Forced Oscillation Test Mechanism	21
10.	Photographs of VKF 1.C Forced Oscillation Test Mechanism	
	a. Overall View	21
	b. Close-up View of Balance Assembly	21
11.	Location of Base Pressure Orifices	22
12.	Data Verification Plots	23

Page

II. TABLES

1. Configuration Identification 25
2. Model Boundary Layer and Trip Effectiveness Run Summary 26
3. Support Interference Run Summary 27
4. Estimated Uncertainties
   a. Basic Steady-State Measurements 31
   b. Basic Dynamic Measurements 32
   c. Calculated Parameters 33

III. SAMPLE OF TABULATED AND PLOTTED DATA

1. Tabulated Summary Data 37
2. Plotted Data 38

NOMENCLATURE

A	Reference area, model base area, 0.3491 ft^2
ALFI	Model support angle of attack, deg
ALPHA	Model angle of attack, deg
ALPHAD	Time rate of change of ALPHA, radians/sec
BETA	Model sideslip angle, deg
CLMA	Slope of the pitching-moment curve, $radian^{-1}$
CLMQ	Damping-in-pitch derivatives, $\partial CLMT/\partial (Q'D/2V) + \partial CLMT/\partial (ALPHAD \cdot D/2V)$, $radian^{-1}$
CLMT	Pitching-moment coefficient, pitching moment/QAD
CONFIG	Model configuration number
D	Reference length, model base diameter, 0.6667 ft
GAMMA	Phase angle between the forcing moment and the angular displacement, deg
INERTIA	Model moment of inertia about the pivot axis, 0.408 slug-ft^2
K	Average height of carborundum grit used on boundary layer trip (if zero, no trip is used), in.
L	Reference length, model base diameter, 0.6667 ft
LP	Distance between model base and beginning of plate, ft
LS	Distance between model base and sting flare, ft
M	Free-stream Mach number
MTF	Angular restoring moment of the cross-flexure pivot, ft-lb/rad
OMEGA-W	Wind-on angular frequency, radians/sec
P	Free-stream static pressure, psi or psf
PB, PB1, PB2	Ratio of base pressure to free-stream static pressure
PHIB	Balance roll angle, deg

PHIM	Model roll angle, deg
PHII	Model support roll angle, deg
PLATE	Plate number used (if zero, no plate is used)
PT	Free-stream total pressure, psfa
Q	Free-stream dynamic pressure, psf
Q'	Pitching velocity, radians/sec
RE	Free stream unit Reynolds number, ft^{-1}
RED	Free-stream Reynolds number based on D
RFP	Reduced frequency parameter (OMEGA-W•D)2V, radian
RUN	Run number
THETA	Wind-on oscillation amplitude, ±deg
TT	Free-stream total temperature used in data reduction, deg R
V	Free-stream velocity, ft/sec

1.0 INTRODUCTION

The work reported herein was sponsored by the Arnold Engineering Development Center (AEDC), Air Force Systems Command (AFSC), Arnold Air Force Station, Tennessee, under Program Element 65807F, and Control Number 9R02-00-9. The results were obtained by ARO, Inc., AEDC Division (a Sverdrup Corporation Company), operating contractor for the AEDC. The test was conducted in the Propulsion Wind Tunnel Facility (PWT), Aerodynamic Wind Tunnel (4T) under ARO Project No. P41C-A9 from September 26 to October 3, 1979. This test provided data in support of the research project "AEDC Dynamic Stability Research," ARO Project Number V32F-09. The AEDC Research Monitor was Mr. Alexander F. Money, and the Test Project Monitor was Mr. Bob L. Uselton of ARO, Inc. This work is a continuation of the work reported in Refs. 1 and 2.

The objective of the test was to determine sting-support interference effects on the measurements of static and dynamic stability derivatives and base pressure. This included: (1) defining critical sting length by the measurement of pitch-damping derivatives for two frequencies of oscillation, (2) investigating the effect of sting length on yaw-damping derivatives as a function of angle of attack, and (3) investigating the effect of splitter plates, located behind the model, on pitch damping derivatives.

The model was a 15 percent spherically blunt 7 deg cone. Data were obtained at a constant model oscillation amplitude of ± 1 deg, using the VKF (von Karman Facility) 1.C Forced Oscillation Test Mechanism. Two frequencies of oscillation, nominally 5.6 Hz and 3.1 Hz, were tested. At the high frequency, both pitch-damping and yaw-damping data were obtained as a function of angle of attack (0 to 28 deg) at Mach numbers 0.2 to 1.3. At the low frequency, pitch-damping data were obtained at angles of attack of 0 to 20 deg at Mach numbers 0.2 to 0.9. The effective sting length was varied from 1 to 3.4 model diameters by extending a conical flare to various stations along the sting. Two model wake splitter plates were also investigated. The Reynolds number based on model diameter ranged from 0.2×10^6 to 3.6×10^6 and the reduced frequency parameter varied from 0.006 to 0.049.

A microfilm copy of the final data has been retained in the PWT at AEDC. Inquiries to obtain copies of the test data should be addressed to AEDC/DOT, Arnold Air Force Station, Tennessee 37389.

2.0 APPARATUS

2.1 TEST FACILITY

The Aerodynamic Wind Tunnel (4T) is a closed-loop, continuous flow, variable-density tunnel in which the Mach number can be varied from 0.1 to 1.3 and can be set at discrete Mach numbers of 1.6 and 2.0 by placing nozzle inserts over the permanent sonic nozzle. At all Mach numbers, the stagnation pressure can be varied from 400 to 3400 psfa. The test section is 4-ft square and 12.5 ft long with perforated, variable porosity

(0.5- to 10-percent open) walls. It is completely enclosed in a plenum chamber from which the air can be evacuated, allowing part of the tunnel airflow to be removed through the perforated walls of the test section. The model support system consists of a sector and boom attachment which has a pitch angle capability of -7.5 to 28 deg with respect to the tunnel centerline and a roll capability of -180 to 180 deg about the sting centerline. A more complete description of the tunnel may be found in Ref. 3.

2.2 TEST ARTICLE

The model was a flat base 7-deg half angle cone with a nose bluntness ratio (nose diameter to base diameter) of 15 percent. The moment reference axis was located on the model pivot axis at 60.9 percent of the model length aft of the model nose. The model was constructed of stainless steel and had a total weight of 30.4 lbs and a moment of inertia about the pivot axis of 0.408 slug-ft^2. A sketch of the model and external dimensions is shown in Fig. 1.

Rings of stainless steel coated with carborundum grit were used as boundary layer trips at some of the test conditions. These trip rings were spotwelded to the model just behind the model nose. Trip details and the location on the model are shown in Fig. 2.

The model, when mounted to the Test Mechanism (described in Section 2.3 below), had an effective sting length of 3.4 model diameters and an effective sting-to-model diameter ratio at the model base of 0.22. The effective sting length was shortened by positioning a conical flare (Fig. 3) at 3.3, 3.0, 2.5, 2.0, 1.5, or 1.0 model diameters to the rear of the model base. The flare was mounted to the motor housing such that it did not touch the sting forward of the motor housing. This eliminated the possibility of the flare's changing the sting frequency characteristics or model tare damping. This sting configuration and the associated conical flare components were designed and bulit at AEDC by the VKF, and were also used during the Ref. 1 and 2 tests.

Two types of model wake splitter plates, which attached to the conical flare, were also investigated. A circular clamp was attached to the long plates (No. 8 Plates) to minimize vibration at the forward end of the plates. Neither the clamp or the plates touched the sting. Plate details are shown in Fig. 4, and plate installation details are shown in Figs. 5 and 6.

A sketch of the model installation is presented in Fig. 7. A photograph showing a typical model-sting configuration in the test section is shown in Fig. 8.

2.3 TEST MECHANISM

The VKF 1.C Forced Oscillation Test Mechanism (Figs. 9 and 10) utilizes a cross flexure pivot, an electric shaker motor and a one-component moment beam which is instrumented with strain gages to measure the forcing moment of the shaker motor. The motor is coupled to the moment beam by means of a connecting rod and flexural linkage which

convert the translational force to a moment to oscillate the model at amplitudes up to ±3 deg (depending on flexure balance) and frequencies from 2 to 8 Hz. The cross flexures, which are instrumented to measure the pitch/yaw displacement, support the model loads and provide the restoring moment to cancel the inertia moment when the system is operating at its natural frequency. The moment beam is not subjected to the static loads, and can be made as sensitive as required for the dynamic measurements.

Two different sets of cross flexure pivots were used to obtain data at the high and low oscillation frequencies. The high frequency (≈ 5.6 Hz) was obtained with the 0.150 in. thick cross flexures, having a stiffness of 466 ft-lb/rad. These were used for Runs 4 to 199, inclusive. The low frequency (≈3.1 Hz) was obtained with the 0.100 in. thick cross flexures, having a stiffness of 141 ft-lb/rad. These were used for Runs 200 to 270, inclusive. The same moment beam was used throughout the entire test. It has a thickness of 0.046 in., and is capable of measuring a total moment of 9.8 inch-lbs.

The cross flexure pivot, moment beam, and flexural linkage assembly, which is referred to as the Balance Assembly (Fig. 10b), is supported by a long, slender cylindrical sting with a 1 deg taper. The sting is instrumented with strain gages to measure the static and oscillatory deflections of the sting in both the pitch and yaw planes.

A penumatic- and spring-operated locking device is provided on the balance to hold the model during tunnel start-up and shut-down. More detailed information regarding the VKF 1.C Forced Oscillation Test Mechanism may be found in Ref. 2.

2.4 TEST INSTRUMENTATION

2.4.1 Forced Oscillation Instrumentation

The forced-oscillation instrumentation (Ref. 4) utilizes an electronic analog system with precision electronics. The control, monitor, and data acquisition instrumentation are contained in a portable console that can be easily interfaced with the instrumentation of the various wind tunnels at AEDC.

The control instrumentation provides a system which can vary the oscillation amplitude of the model within the flexure limits. The oscillation amplitude is controlled by an electronic feedback loop which permits testing of both dynamically stable and unstable configurations.

Data are normally obtained at or near the natural frequency of the model flexure system; however, the electronic resolvers permit data to

be obtained off resonance. All gages are excited by d-c voltages, and outputs are increased to optimum values by d-c amplifiers. Typical balance outputs from an oscillating model are composed of oscillatory components (OC) superimposed on static components (SC). These components are separated by bandpass and lowpass filters. The SC outputs are used to calculate the static moment coefficients and static sting deflections. The OC outputs are input to the resolver instrumentation and precise frequency measuring instrumentation. The resolvers utilize very accurate analog electronic devices to process the OC signals and output d-c voltages. The output d-c voltages are porportional to the amplitude squared, the in-phase and quadrature (90 deg out-of-phase) balance components (forcing torque), and the in-phase and quadrature sting components. An analog-to-digital (A/D) converter converts these outputs to digital signals. The data are recorded for a period of time selected from approximately 2 to 60 sec at a sample rate appropriate for the type test and wind tunnel.

2.4.1 Model Base Pressure Instrumentation

Model base pressures were measured with 2 Sunstrand (Kistler) 314D Servo pressure transducers located on the tunnel plenum chamber wall. The locations of the orifices with respect to the model and sting are shown in Fig. 11.

3.0 TEST DESCRIPTION

3.1 TEST CONDITIONS AND PROCEDURES

3.1.1 General

A summary of the nominal test conditions at each Mach number is listed below.

M	PT, psfa	TT, deg R	Q, psf	P, psf	V, ft/sec	$RE\times10^{-6}, ft^{-1}$	$RED\times10^{-6}$
0.2	400	554	11	389	230	0.24	0.16
	820*	550	22	797	230	0.50	0.33
	2000	566	54	1945	232	1.18	0.78
	3200	586	87	3112	236	1.81	1.20
	3600*	593	98	3501	238	2.00	1.33
0.4	870	553	87	779	454	1.00	0.67
0.6	410	558	81	321	671	0.64	0.43
	1300	549	257	1019	666	2.08	1.39
	1630*	569	322	1278	678	2.50	1.66
	3200*	581	632	2508	685	4.77	3.18
0.8	1320	555	388	866	870	2.49	1.66
0.9	1260*	556	422	745	965	2.49	1.66
	2800*	603	939	1656	1005	5.00	3.33
0.95	800	550	283	448	1005	1.64	1.09
	1020	554	360	571	1009	2.07	1.38
	1220	556	431	683	1011	2.46	1.64
	1600	560	565	895	1014	3.20	2.13
	2200	567	778	1231	1021	4.33	2.88
	2800	578	990	1567	1030	5.37	3.58

*Primary Test Conditions

M	PT, psfa	TT, deg R	Q, psf	P, psf	V, ft/sec	$REx10^{-6}, ft^{-1}$	$REDx10^{-6}$
1.10	1200*	555	476	562	1140	2.51	1.67
	2640*	600	1047	1236	1185	4.99	3.33
1.20	1200	556	499	495	1222	2.53	1.68
1.30	1300*	556	555	469	1299	2.73	1.82
	1600	568	683	577	1313	3.26	2.17
	2200	578	939	794	1325	4.39	2.92
	2560*	588	1093	924	1336	4.99	3.33
	2700	591	1153	974	1339	5.23	3.48

*Primary Test Conditions

The reduced frequency parameter at the high oscillation frequency (≈5.6 Hz) ranged from 0.008 radians at Mach number 1.3, to 0.049 radians at Mach number 0.2. At the low oscillation frequency (≈3.1 Hz), it ranged from 0.006 radians at Mach number 0.9, to 0.027 radians at Mach number 0.2.

The variables for each configuration are listed in Table 1. The Test Summaries, which contain all configurations tested and the variables for each, are shown in Tables 2 and 3. Table 2 contains the summary of the model boundary layer and trip effectiveness investigation (Runs 26 to 46), and Table 3 contains the summary of the support interference investigation (Runs 49 to 269).

Testing procedures in the yaw oscillation plane were identical to those in the pitch plane, except that the entire forced oscillation mechanism was rolled +90 deg (PHIB = 90).

3.1.2 Data Acquisition

After establishing tunnel conditions and model attitude, the model was unlocked, and brought to a constant oscillation amplitude of ±1 deg by using the Forced Oscillation Control System. The system was allowed to stabilize at the system resonant frequency before data were recorded. At each angle of attack, generally two data points were taken. Data were obtained over a 60 second time interval at each data point. The balance and sting gage outputs and frequency instrumentation were read from the forced oscillation instrumentation console by a Digital Data Acquisition System (DDAS), at a rate of approximately 54 samples per second.

The Automatic Model Attitude Positioning System (AMAPS) was used to control the model position. A list of model angle of attack requirements were programmed into the AMAPS prior to the test. After data were obtained at a given angle of attack, the AMAPS was manually activated, and the model was automatically pitched to the next angle of attack on the AMAPS list.

3.2 DATA REDUCTION

Data from the DDAS were combined with tunnel model attitude and base pressure instrumentation data and sent directly to a DEC-10 System Computer. Average values of the balance and sting gage outputs were

calculated by the computer, and used in conjunction with the remaining DDAS outputs to calculate the dynamic derivatives. Both the SC and OC sting gage outputs were used to correct the data for sting bending effects. The method used to reduce the data is given in Refs. 4 and 5.

A print-out of each reduced data point was obtained approximately 2 minutes (Real Time) after the DDAS sent the unreduced data to the computer. Summary data were printed-out at the conclusion of each angle of attack sweep. Reduced data were also plotted during the test, using the IBM-370 computer Interactive Graphics System, which received the reduced data from the DEC-10. Usually, the data were available for plotting on the IBM-370 Graphics System within the same amount of time (2 minutes Real Time) as the reduced data print-out. This enabled close monitoring of the data during the angle of attack sweep, and allowed cross plots (cross checks) to be made with similar configurations obtained earlier in the test.

3.3 UNCERTAINTY OF MEASUREMENTS

In general, instrumentation calibrations and data uncertainty estimates were made using methods recognized by the National Bureau of Standards. Measurement uncertainty is a combination of bias and precision errors defined as:

$$U = \pm (B + t_{95} S)$$

where B is the bias limit, S is the sample standard deviation, and t_{95} is the 95th percentile point for the two-tailed Student's "t" distribution, which for degrees of freedom greater than 30 is equal to 2.

Estimates of the measured data uncertainties for this test are given in Table 4a. With the exception of the Test Mechanism, data uncertainties are determined from in-place calibrations through the data recording system. Static load hangings on the Forced Oscillation Mechanism simulated the range of loads and deflections anticipated during the test, and measurement errors are based on differences between applied loads and deflections and corresponding values calculated from the mechanism calibration. Load hangings to verify the sting and balance calibrations are made in the tunnel prior to testing using a special calibration model.

Propagation of the bias and precision errors of measured data through the calculated data were made in accordance with Ref. 6. Uncertainties in the calculated tunnel parameters are given in Table 4b, and uncertainties in the dynamic parameters are given in Table 4c.

The quoted uncertainties are based upon steady-state operation and do not reflect the effects of the wind tunnel environment. In some instances the damping data (CLMQ) will show slightly larger scatter in the repeatability, usually on the order of about 5-10 percent. Also, the large quoted uncertainties for CLMA are the result of the small magnitude of the measurement and the fact that the wind-on measurement level is about the same level as the wind-off measurement (particularly at lower angles of attack).

4.0 DATA PACKAGE PRESENTATION

The Data Package includes tabulated and plotted data, data notes, run logs, and nomenclature. The tabulated data includes summary data, point-by-point data, wind-off tare data, and torque calibration data. Plotted data include (1) individual plots of CLMQ, CLMA, CLMT, and PB2 as functions of angle of attack, and (2) comparison plots which depict sting length ratio (LS/D), Reynolds number, frequency, and splitter plates effects. A sample of the Tabulated Data and Plotted Data is presented in Appendix III.

Verification plots of the pitch-damping data and base pressure ratio data are shown in Fig. 12. The plots indicate good agreement between the extrapolation of the present results ($0.2 \leq M \leq 1.3$) and the previous supersonic-hypersonic results ($2.0 \leq M \leq 8$) reported in Refs. 1 and 2.

REFERENCES

1. Uselton, B. L. and Cyran, F. B. "Critical Sting Length as Determined by the Measurement of Pitch-Damping Derivatives for Laminar, Transitional, and Turbulent Boundary Layers at Mach Number 3 for Reduced Frequencies of 0.0033 and 0.0056," AEDC-TR-77-66, July 1977.

2. Uselton, B. L. and Cyran, F. B. "Sting Interference Effects as Determined by Measurements of Dynamic Stability Derivatives, Surface Pressure, and Base Pressure for Mach Numbers 2 through 8," AEDC-TR-79-89, to be published.

3. Test Facilities Handbook (Eleventh Edition). "Propulsion Wind Tunnel Facility, Vol. 4." Arnold Engineering Development Center, June 1979.

4. Burt, G. E. "A Description of a Pitch/Yaw Dynamic Stability, Forced Oscillation Test Mechanism for Testing Lifting Configurations." AEDC-TR-73-60, June 1973.

5. Schueler, C. J., Ward, L. K., and Hodapp, A. E., Jr. "Techniques for Measurements of Dynamic-Stability Derivatives in Ground Test Facilities." AGARDograph 121 (AD669227), October 1967.

6. Thompson, J. W. and Abernethy, R. B. et al. "Handbook Uncertainty in Gas Turbine Measurements." AEDC-TR-73-5 (AD755356), February 1973.

APPENDIX I

ILLUSTRATIONS

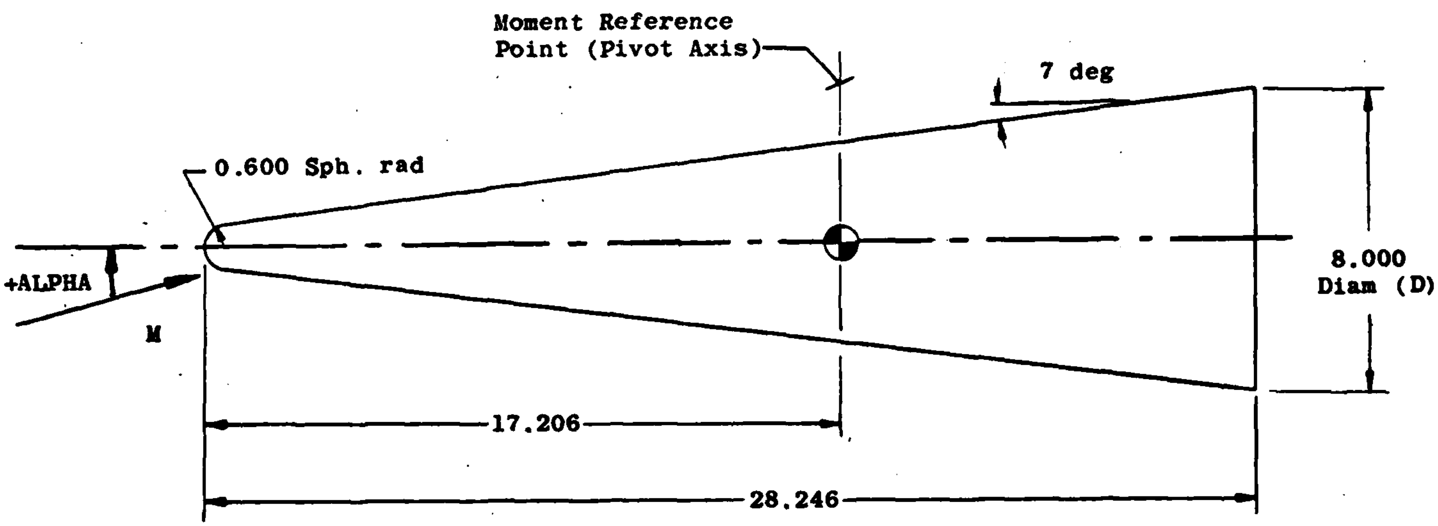

All Dimensions in Inches

Fig. 1. Model details

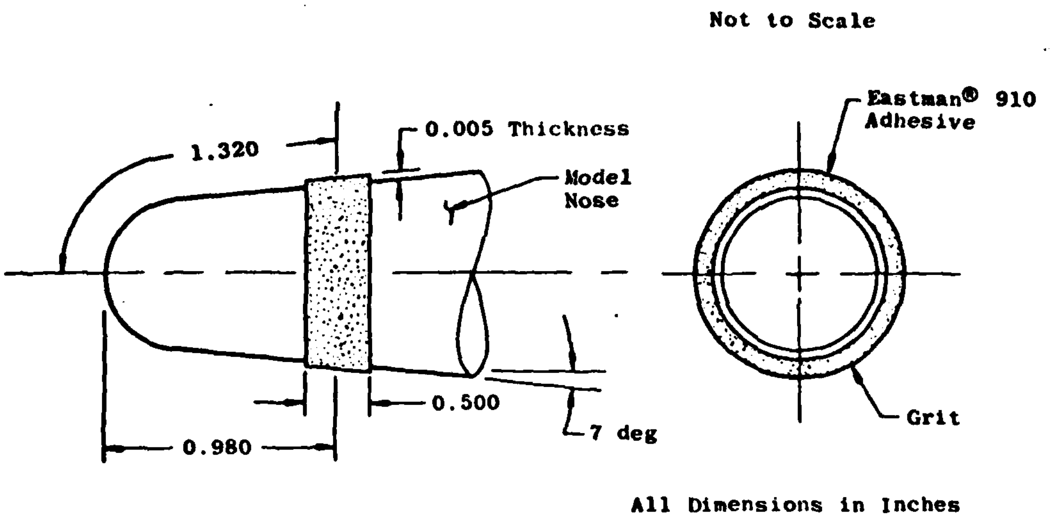

Trip	Grit Size	Average Height of Grit, in.
1	#60	0.012
2	#36	0.020

Fig. 2. Boundary layer trip details.

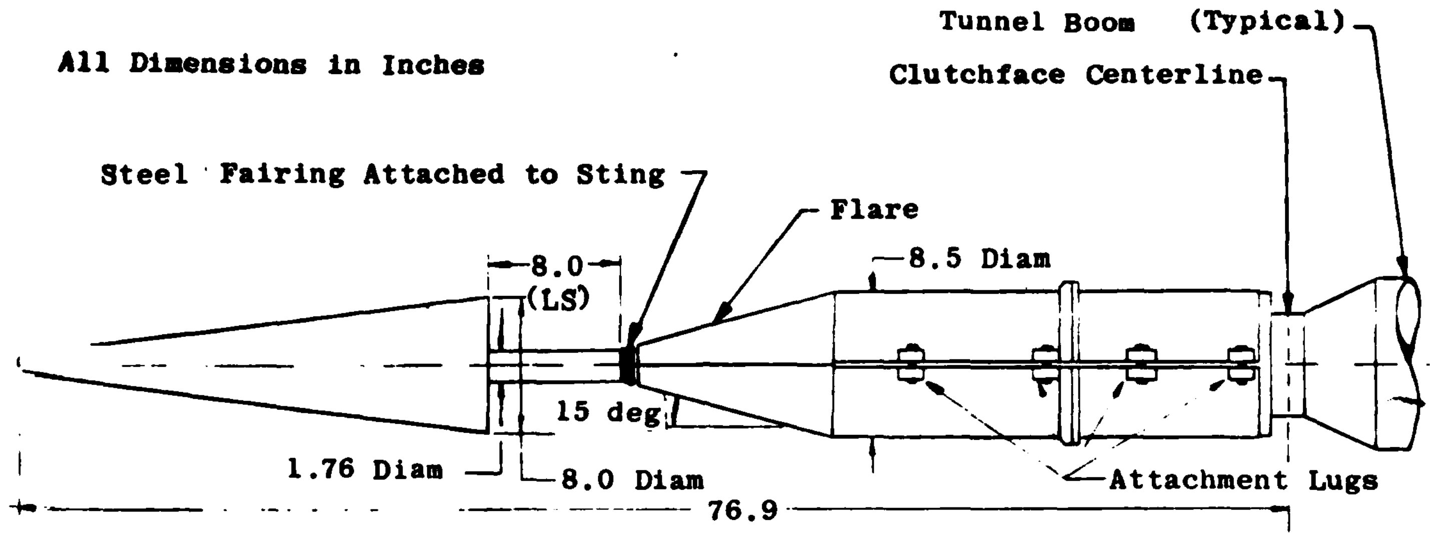

a. Interference sting, LS/D = 1.0

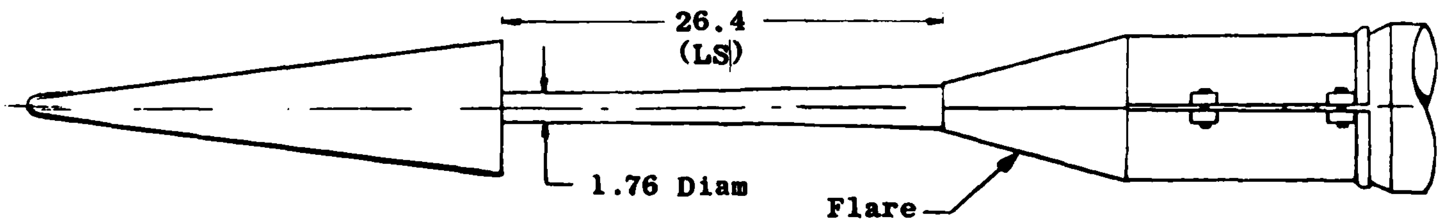

b. Clean sting, LS/D = 3.3

Fig. 3. Details of model support configurations.

All Dimensions in Inches

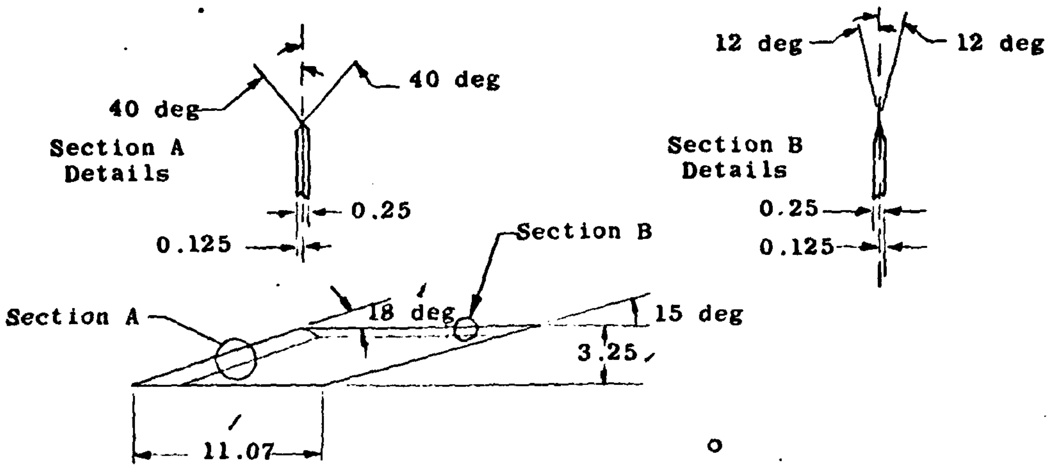

a. Plate 1

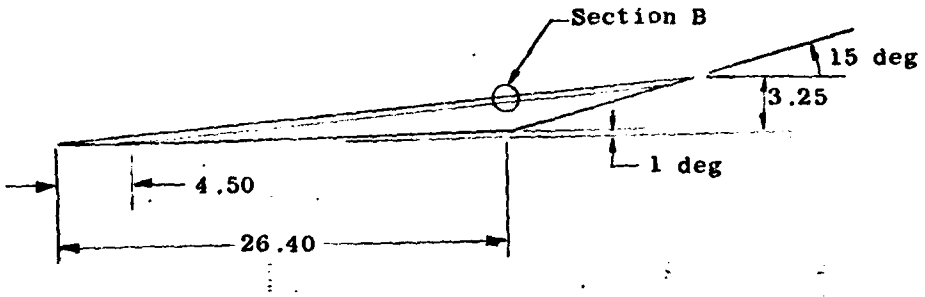

b. Plate 8

Fig. 4 Splitter Plate Details

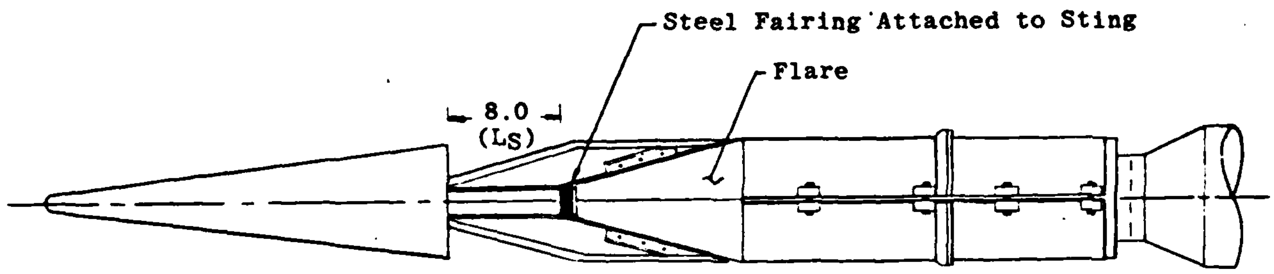

a. Plate 1 installed, $L_S/D = 1.0$

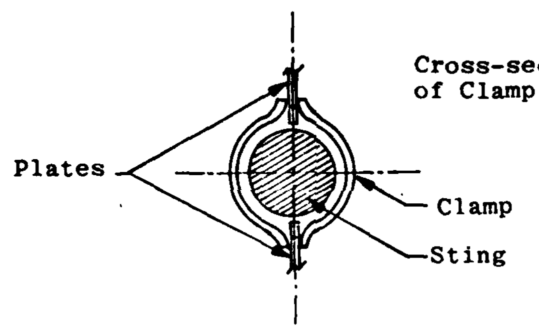

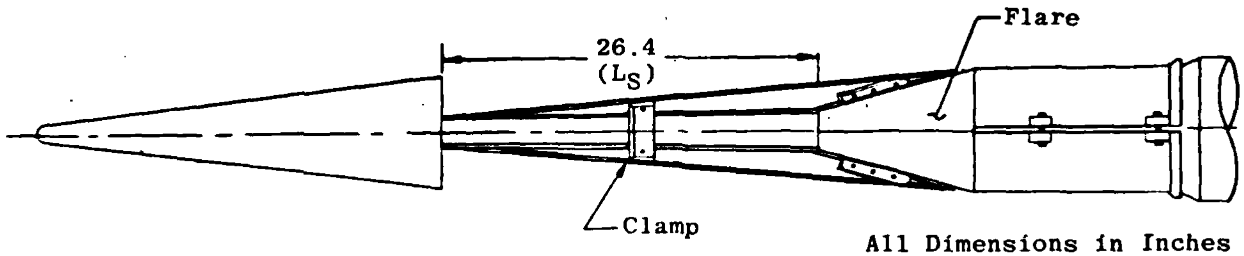

b. Plate 8 installed, $L_S/D = 3.3$

Fig. 5. Details of Splitter Plate Configurations.

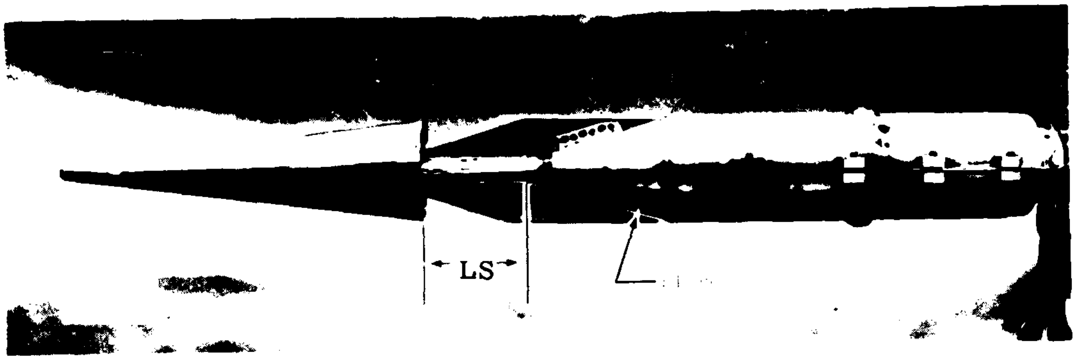

a. Plate 1 installed, LS/D = 1.0

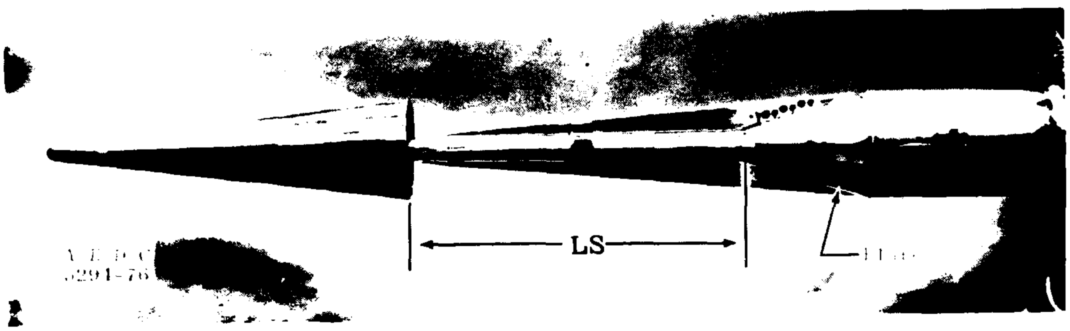

b. Plate 8 installed, LS/D = 3.3

Fig. 6 Photographs of Splitter Plate Installation

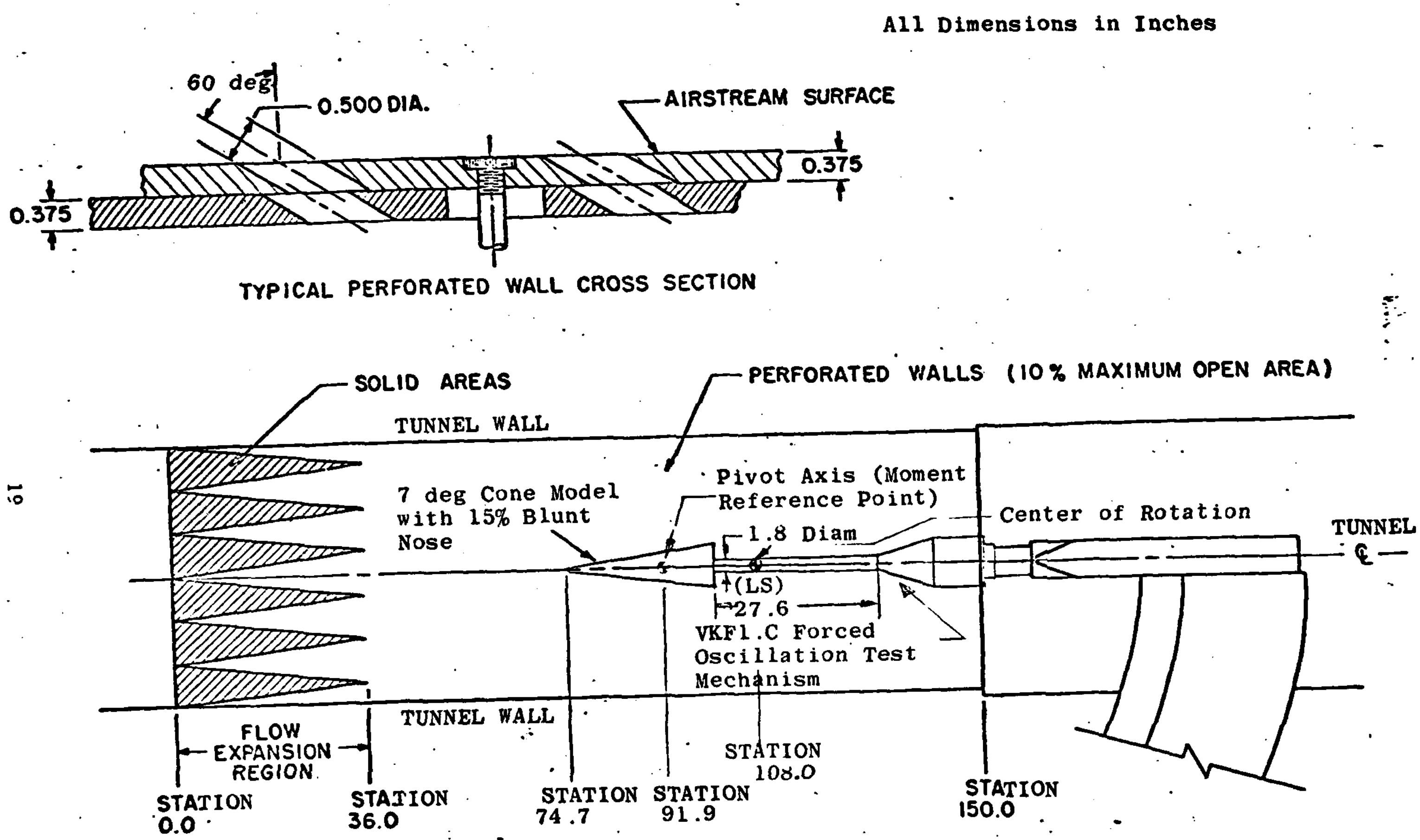

Fig. 7. Model Installation Sketch in PWT Aerodynamic Wind Tunnel (4T)

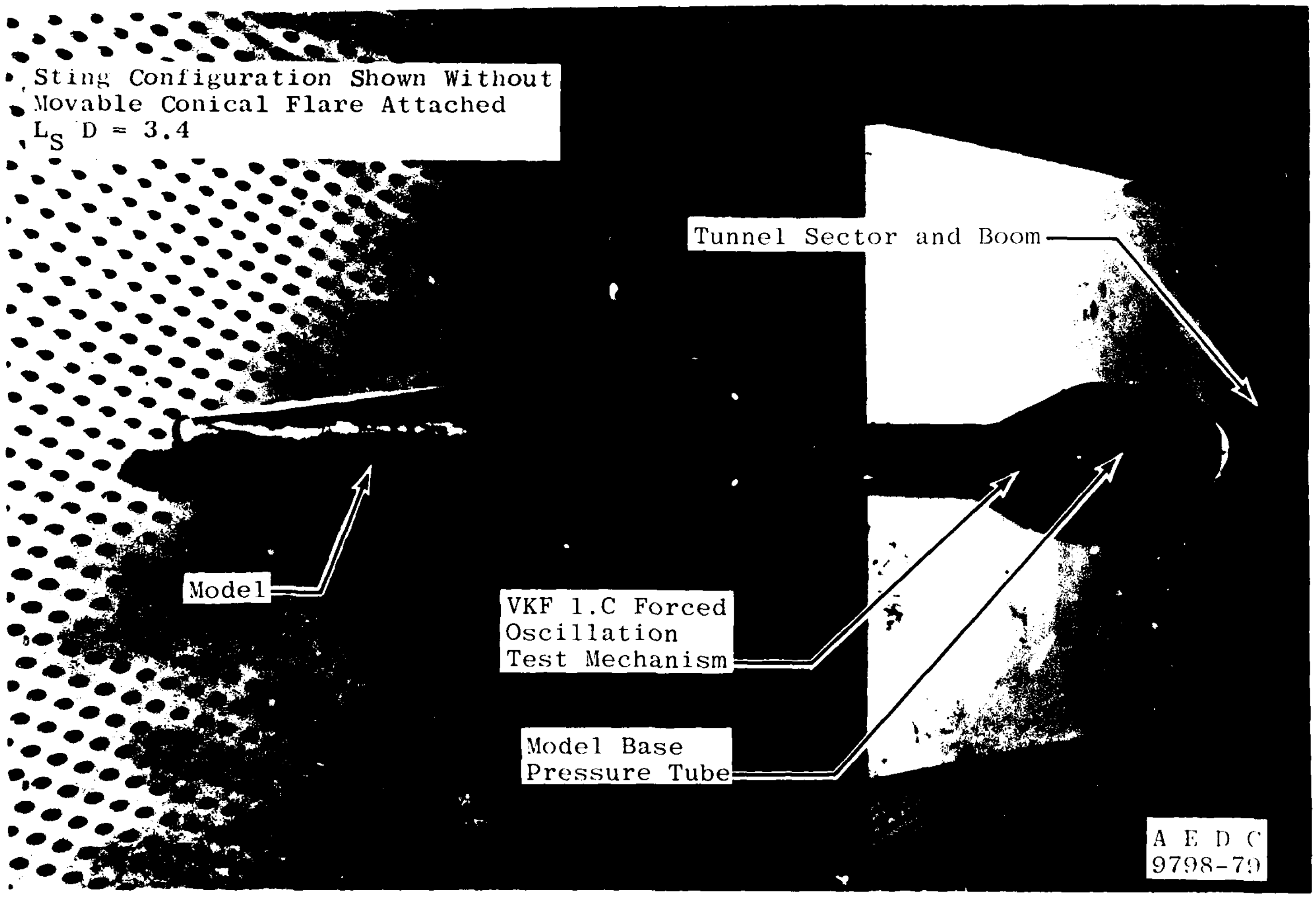

Figure 8. Photograph of Model Installation in PWT Wind Tunnel (4T)

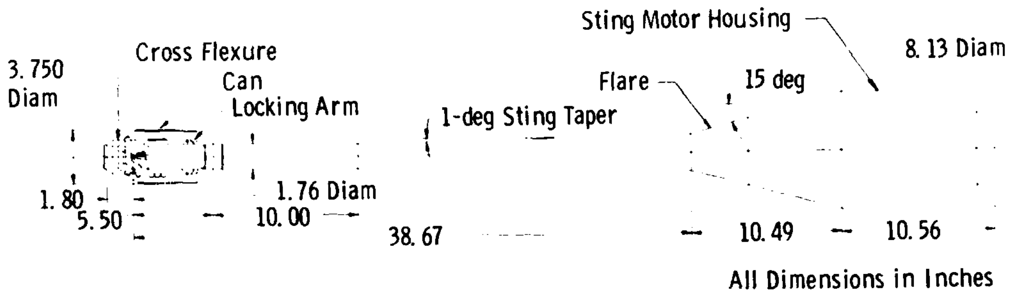

Fig. 9. Details of VKF 1.C Forced Oscillation
Test Mechanism

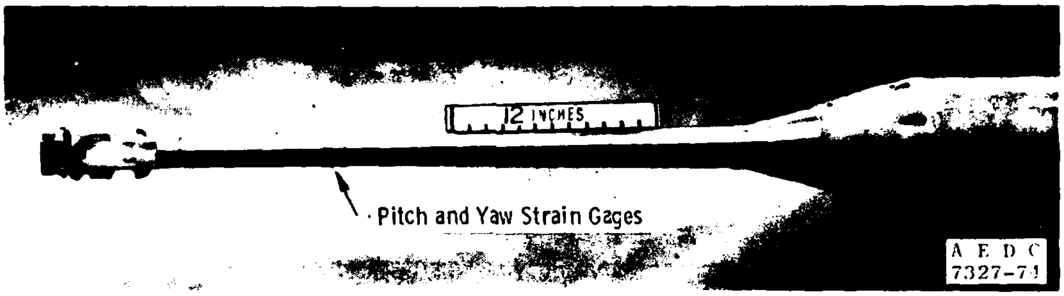

a. Overall View

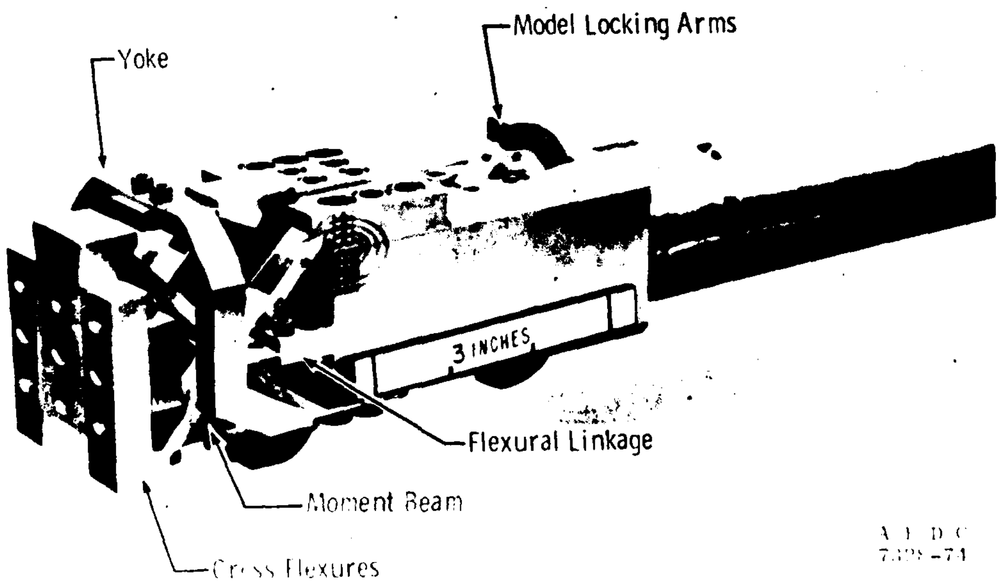

b. Close-Up View of Balance Assembly
Fig. 10. Photographs of VKF 1.C Forced Oscillation
Test Mechanism

All Dimensions in Inches

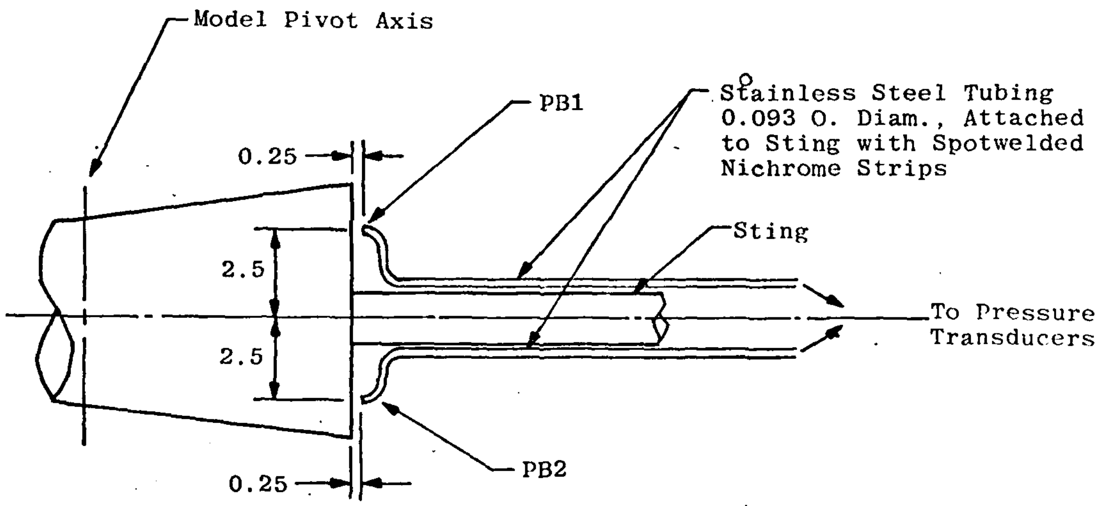

Orifice Diameter = 0.062 I. Diam.

Top View - Looking Down on Model from the Tunnel Top Wall

Fig. 11. Location of Base Pressure Orifices

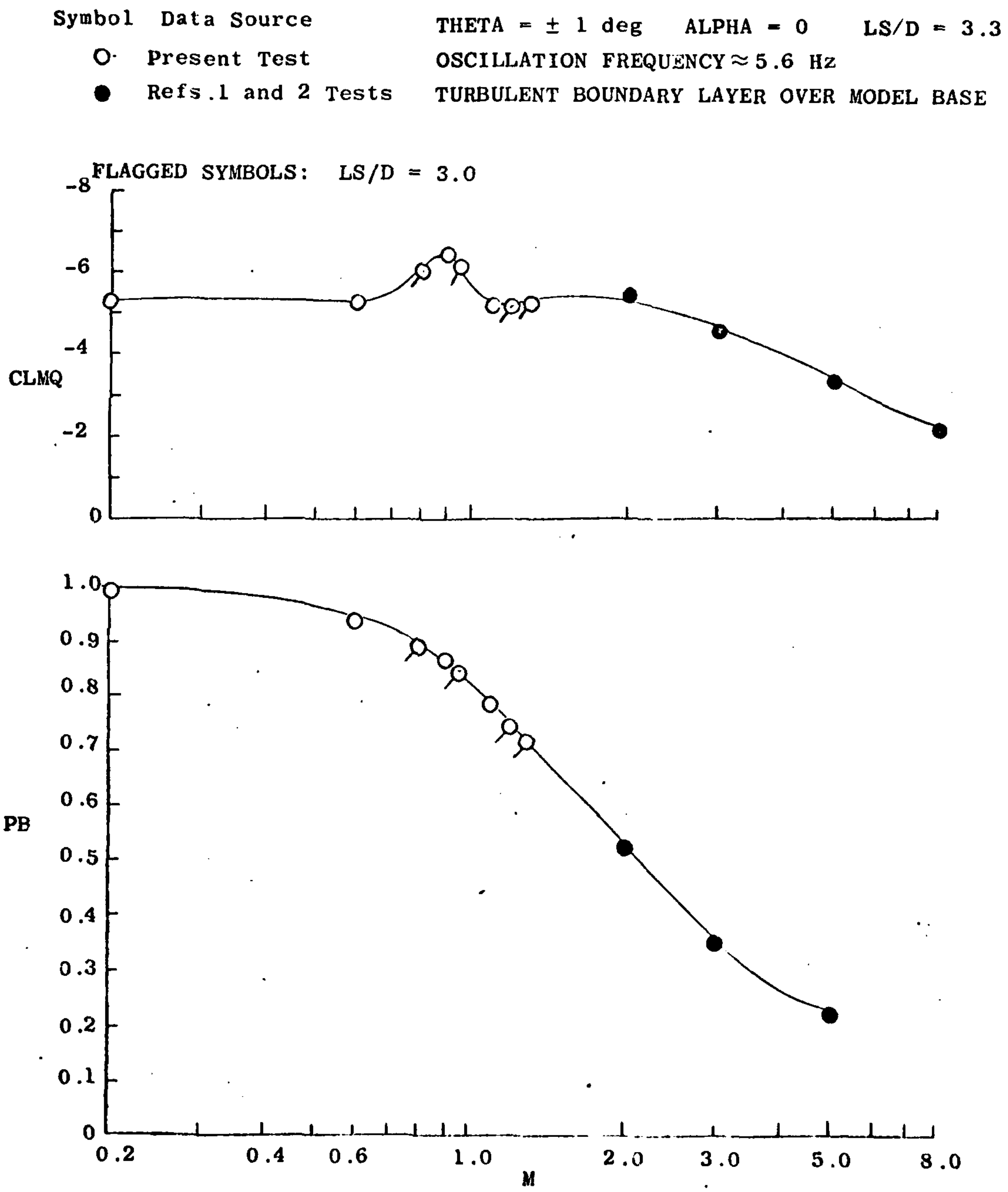

Fig. 12. Data Verification Plots

APPENDIX II

TABLES

TABLE 1. CONFIGURATION IDENTIFICATION

CONFIGURATION	LS/D	MTF	FREQUENCY,Hz
1	3.4	466	5.6
2	3.3		
2A	3.0		
3	2.5		
4	2.0		
5	1.0		
6	1.5		
19	3.3	141	3.1
19A	3.0		
20	2.5		
21	2.0		
22	1.0		
23	1.5		

TABLE 2. MODEL BOUNDARY LAYER AND TRIP EFFECTIVENESS
RUN SUMMARY

CONFIG 1 LS/D = 3.4 PITCH OSCILLATION

OSCILLATION FREQUENCY ≈5.6 Hz

RUN	M,	PT, psfa	RED×10⁻⁶	BOUNDARY LAYER TRIP No.	K, in	ALPHA, deg
26	0.60	1300	1.4	NONE	—	0
27		1300	1.4			15
28		1300	1.4			0,15,26
29		3200	3.2			0,25
30	↓	410	0.4			0
31	0.95	1020	1.4			↓
32		1020	1.4			0→24
33		1020	1.4			0
		2800	3.6			
		2200	2.9			
		1600	2.1			
	↓	800	1.1			
34	1.30	1300	1.8			
		2200	2.9			
	↓	2700	3.5			
35	0.20	3200	1.2			
		2000	0.8			
		400	0.2	↓	↓	
40	↓	3200	1.2	2	0.020	
41	0.95	2800	3.3			
42	1.30	2700	3.5			
	↓	2200	2.9	↓	↓	
45	0.95	2800	3.3	1	0.012	
46	1.30	2700	3.5			
	↓	1600	2.2	↓	↓	↓

TABLE 3

SUPPORT INTERFERENCE RUN SUMMARY

NO TRIPS USED

RUN	SPLITTER PLATE No.	CONFIG	LS/D	M_∞	$RED \times 10^{-6}$	OSCILLATION PLANE	RFP, per rad.	ALPHA, deg
49	NONE	2A	3.0	0.95	1.4	PITCH	0.011	0→24
50					1.6			0
51				↓	1.6		↓	0→20
52				0.20	0.3		0.049	0
53				0.40	0.7		0.025	
54				0.60	1.7		0.016	
55				0.80	1.7		0.013	↓
56				0.80	1.7		0.013	0→20
64				0.90	1.7		0.012	0→20
65				1.10	1.7		0.010	0
66				1.20	1.8		0.009	0
67		↓	↓	1.30	1.8		0.009	0→20
71		3	2.5	0.20	0.3		0.049	0
72				0.60	1.7		0.016	
73				0.90	1.7		0.012	
74				1.10	1.7		0.010	
75		↓	↓	1.30	1.8		0.009	↓
79		5	1.0	0.20	0.3		0.049	0→20
80				0.40	0.7		0.025	0
81				0.60	1.7		0.017	0, 4
83				0.60	1.7		0.017	0→20
84				0.80	1.7		0.013	0
85				0.90	1.7		0.012	0→20
87				1.10	1.7		0.010	0→20
88				1.20	1.8		0.009	0
89				1.30	1.8		0.008	0→20
90				1.30	3.3		0.008	0
91				0.90	3.3		0.011	
92				1.10	3.3		0.009	
93				0.60	3.2		0.016	
94	↓	↓	↓	0.20	1.3	↓	0.047	↓

TABLE 3. Continued

NO TRIPS USED

RUN	SPLITTER PLATE No.	CONFIG	LS/D	M,	RED×10⁻⁶	OSCILLATION PLANE	RFP, per rad.	ALPHA, deg
98	NONE	4	2.0	0.20	0.3	PITCH	0.048	0
99				0.60	1.7		0.016	
100				0.60	1.7		0.016	
101				0.90	1.7		0.012	
102				1.10	1.7		0.010	
103				1.30	1.8		0.009	
104				1.30	3.3		0.008	
105				1.30	3.3		0.008	
106				1.10	3.3		0.009	
107				0.90	3.3		0.011	
108				0.60	3.2		0.016	
109				0.20	1.3		0.046	
113		6	1.5	0.20	0.3		0.048	0 → 20
114				0.60	1.7		0.016	
115				0.90	1.7		0.012	
116				1.10	1.7		0.010	0
117				1.30	1.8		0.008	0 → 20
118				1.10	3.3		0.009	0
119				0.20	1.3		0.046	0 → 20
123		3	2.5	1.10	1.7		0.010	0
128		2	3.3	0.60	1.7		0.017	0 → 20
129				0.90	1.7		0.012	0
130				0.90	1.7		0.012	12, 20
131				1.10	1.7		0.010	0
132				1.10	1.7		0.010	0 → 20
137		5	1.0	0.60	1.7	YAW	0.017	
139				1.10	1.7		0.010	
141				1.30	1.8		0.008	
145		2A	3.0	1.10	1.7		0.010	
147				1.30	1.8		0.009	
148				0.60	1.7		0.017	

TABLE 3. Continued
NO TRIPS USED

RUN	SPLITTER PLATE No.	CONFIG	LS/D	M,	RED×10^{-6},	OSCILLATION PLANE	RFP, per rad	ALPHA, deg
160	NONE	2	3.3	0.20	0.3	PITCH	0.050	0→20
161				0.60	1.7		0.016	0
162				0.60	1.7		0.016	0→20
163				0.90	1.7		0.012	
166	8			0.20	0.3		0.049	
167				0.60	1.7		0.016	
168				0.90	1.7		0.012	
204	NONE	19		0.20	0.3		0.027	0→16
205				0.20	0.3		0.027	4,20
206				0.60	1.7		0.009	0→20
207				0.60	1.7		0.009	0
208				0.90	1.7		0.006	0→20
212		21	2.0	0.20	0.3		0.027	0→20
213				0.60	1.7		0.009	0
214				0.90	1.7		0.006	0
217		22	1.0	0.20	0.3		0.027	0→20
218				0.60	1.7		0.009	0→20
233				0.20	0.3		0.027	0
234				0.20	1.3		0.027	0
235				0.60	3.2		0.009	0
236				0.60	1.7		0.009	0→20
237				0.90	1.7		0.006	0→20
241	1			0.20	0.3		0.027	0,4,8
252				0.20	0.3		0.027	0→20
253				0.60	1.7		0.009	0,12,20
254				0.90	1.7		0.006	0,12,20
257	NONE	23	1.5	0.20	0.3		0.027	0
258				0.60	1.7		0.009	
259				0.90	1.7		0.006	
262		20	2.5	0.20	0.3		0.027	
263		20	2.5	0.60	1.7		0.009	

TABLE 3. Concluded

NO TRIPS USED

RUN	SPLITTER PLATE No.	CONFIG	LS/D	M,	$RED \times 10^{-6}$	OSCILLATION PLANE	RFP, per rad	ALPHA, deg
264	NONE	20	2.5	0.90	1.7	PITCH	0.006	0
267		19A	3.0	0.20	0.3		0.027	
268				0.60	1.7		0.009	
269				0.90	1.7		0.006	

TABLE 4. ESTIMATED UNCERTAINTIES

a. Basic Steady-State Measurements

Parameter Designation	STEADY-STATE ESTIMATED MEASUREMENT* Precision Index (S) Percent of Reading	Precision Index (S) Unit of Measurement	Precision Index (S) Degree of Freedom	Bias (B) Percent of Reading	Bias (B) Unit of Measurement	Uncertainty $\pm(B + t_{95}S)$ Percent of Reading	Uncertainty $\pm(B + t_{95}S)$ Unit of Measurement	Range	Type of Measuring Device	Type of Recording Device	Method of System Calibration
PT,psfa	±(0.04% + 0.15)	±0.7	30 30	±(0.11% + 1)	±2.9	±(0.2% + 1.3)	±4.3	0 to 1500 1500 to 4000	Datametrics Barocel Model 538AX-93 0-4000 PSFA	Datametrics Electronic Manometer C-1018	In-place calibration with a precision pressure standard
TT,deg R		±0.1	6		±0.55		±0.77	410 to 610	Dual Chromel-Alumel Thermocouples	Newport Model 2600KF Digital Thermometer	Voltage standard substitution using a stirred ice bath thermocouple reference
PB,psfa		±1.0	32	±(0.14% + 1)		±(0.14% + 3)		0 to 2160	Sunstrand(Kistler) 314D Servo Pressure Transducer	Preston Amplifier used with a Preston G-MAD-3 for A/D Conversion	In-place calibration with a precision pressure standard
ALPI,deg	±(0.014% + 0.004)		7		±0.029	±(0.03% + 0.038)		-8 to 27	Clifton Precision Products Model CG-10-AS-1 SYNCHRO Transmitter	Theta Model C-5260 Digital Indicator	In-place calibration by comparison to an inclinometer
PHII,deg		±0.04	7		±0.300		±0.390	±180			
FREQUENCY,Hz	0.0025		2		0	0.01		0 to 10	A/D Frequency Converter Built by VKF	Digital Data Acquisition System(DDAS)	Compared with a Frequency Standard
MODEL ANGULAR DISPLACEMENT ABOUT THE PIVOT AXIS, deg a. 0.10 in. thick cross flexures		0.024	26				0.048	±3	Bonded Strain Gages		Static Loading
b. 0.15 in. thick cross flexures		0.017	32				0.034	±3			
STING ANGULAR DISPLACEMENT,deg		0.006	32				0.014	±1			

*Thompson, J. W. and Abernethy, R. B. et al. "Handbook Uncertainty in Gas Turbine Measurements." AEDC-TR-73-5 (AD 755356), February 1973.

VB-16 (8/79)

TABLE 4. Continued

b. Basic Dynamic Measurements

Parameter Designation	STEADY-STATE ESTIMATED MEASUREMENT[a]							Range	Type of Measuring Device	Type of Recording Device	Method of System Calibration
	Precision Index (S)			Bias (B)		Uncertainty ±(B + t_{95}S)					
	Percent of Reading	Unit of Measurement	Degree of Freedom	Percent of Reading	Unit of Measurement	Percent of Reading	Unit of Measurement				
OUT-OF-PHASE TORQUE, ft-lbs		0.0001	10		0		0.0002	0 to 0.82	Bonded Strain Gages	Digital Data Acquisition System (DDAS)	In-place Moment Loading
IN-PHASE TORQUE, ft-lbs		5.2×10^{-5}	10				0.0001	0 to 0.82			
IN-PHASE STING MOMENT, ft-lbs		0.35	32				0.70	0 to 50			Static Loading
THETA, deg											
a. 0.10 in. thick cross flexures		0.024	26				0.048	±3			
b. 0.15 in. thick cross flexures		0.017	32				0.034	±3			

[a] Thompson, J. W. and Abernethy, R. B. et al. "Handbook Uncertainty in Gas Turbine Measurements." AEDC-TR-73-5 (AD 755356), February 1973.

VB-16 (8/79)

TABLE 4. Continued

c. Calculated Parameters

Parameter Designation	STEADY-STATE ESTIMATED MEASUREMENT* Precision Index (S) Percent of Reading	Precision Index (S) Unit of Measurement	Degree of Freedom	Bias (B) Percent of Reading	Bias (B) Unit of Measurement	Uncertainty $\pm(B + t_{95}S)$ Percent of Reading	Uncertainty $\pm(B + t_{95}S)$ Unit of Measurement	Parameter Range	TEST CONDITIONS M	TEST CONDITIONS RED $\times 10^{-6}$
V, ft/sec		3.5			13.6		20.6	230	0.2	0.3
		1.2			4.9		7.3	238		1.3
		0.9			3.5		5.3	678	0.6	1.7
		0.5			2.0		3.0	685		3.2
		0.7			2.7		4.1	695	0.9	1.7
		0.5			1.8		2.8	1005		3.3
		0.6			2.4		3.6	1140	1.1	1.7
		0.4			1.7		2.5	1185		3.3
		0.5			2.2		3.2	1300	1.3	1.8
		0.4			1.5		2.3	1336		3.3
RED $\times 10^{-6}$		0.005			0.020		0.030	0.3	0.2	
		0.007			0.027		0.041	1.3		
		0.002			0.010		0.014	1.7	0.6	
		[illegible]			[illegible]		[illegible]	[illegible]		
		0.001			0.006		0.008	1.7	0.9	
		0.001			0.009		0.010	3.3		
		0.001			0.006		0.007	1.7	1.1	
		0.001			0.008		0.009	3.3		
		0.001			0.005		0.006	1.8	1.3	
		0.001			0.007		0.008	3.3		
Q, psf		0.66			2.6		3.9	22	0.2	0.3
		0.98			4.0		6.0	98		1.3
		0.81			3.1		4.7	322	0.6	1.7
		0.83			3.4		5.1	632		3.2
		0.53			1.9		3.0	422	0.9	1.7
		0.64			2.6		3.9	938		3.3
		0.40			1.5		2.3	476	1.1	1.7
		0.48			1.9		2.9	1047		3.3
		0.33			1.2		1.8	555	1.3	1.8
		0.35			1.4		2.1	1093		3.3

*Abernethy, R. B. et al. and Thompson, J. W. "Handbook Uncertainty in Gas Turbine Measurements," AEDC-TR-73-5 (AD 755356), February 1973.

VB-16a (9-79)

TABLE 4. Continued

c . Continued

Parameter Designation	STEADY-STATE ESTIMATED MEASUREMENT[a] Precision Index (S) Percent of Reading	Precision Index (S) Unit of Measurement	Degree of Freedom	Bias (B) Percent of Reading	Bias (B) Unit of Measurement	Uncertainty $\pm(B + t_{95}S)$ Percent of Reading	Uncertainty $\pm(B + t_{95}S)$ Unit of Measurement	PARAMETER RANGE	TEST CONDITIONS M	TEST CONDITIONS RED $x10^{-6}$
P,psi		0.003			0.014		0.020	5.5	0.2	0.3
		0.005			0.020		0.030	24.3		1.3
		0.005			0.016		0.026	8.9	0.6	1.7
		0.005			0.020		0.030	17.4		3.2
		0.003			0.013		0.019	5.2	0.9	1.7
		0.005			0.020		0.030	11.5		3.3
		0.003			0.011		0.017	3.9	1.1	1.7
		0.005			0.016		0.026	8.5		3.2
		0.003			0.010		0.016	3.3	1.3	1.8
		0.004			0.014		0.022	6.4		3.3
M		0.003			0.012		0.018	0.2		0.3
		0.001			0.005		0.006	0.2		1.3
		0.001			0.004		0.005	0.6		1.7
		0.001			0.002		0.003	0.6		3.2
		0.001			0.003		0.004	0.9		1.7
		0.001			0.002		0.003	0.9		3.3
		0.001			0.003		0.004	1.1		1.7
		0.001			0.002		0.003	1.1		3.3
		0.001			0.003		0.004	1.3		1.8
		0.001			0.002		0.003	1.3		3.3
ALPHA,deg		0.030			0.040		0.100	0 → 28		

[a]Abernethy, R. B. et al. and Thompson, J. W. "Handbook Uncertainty in Gas Turbine Measurements," AEDC-TR-73-5 (AD 755356), February 1973.

VB-16a (9-79)

TABLE 4. Concluded

c. Concluded

Parameter Designation	STEADY-STATE ESTIMATED MEASUREMENT*							PARAMETER RANGE	TEST CONDITIONS			
	Precision Index (S)			Bias (B)		Uncertainty $\pm(B + t_{95}S)$						
	Percent of Reading	Unit of Measurement	Degree of Freedom	Percent of Reading	Unit of Measurement	Percent of Reading	Unit of Measurement		M	RED $\times 10^{-6}$	ALPHA	RFP
GAMMA, deg		0.4			0.2		1.0	45 → 135				
CLMQ, rad^{-1}	2			6		10		-5.5	0.2	0.3	0	0.049
	1			2		4		-5.4	0.6	1.7	0	0.017
	1			2		4		-5.8	0.9	1.7	0	0.012
	1			2		4		-4.9	1.1	1.7	0	0.010
	[illegible]			2		4		-5.3	1.3	1.8	0	0.009
	3			6		12		-5.0	0.2	0.3	0	0.027
	2			2		6		-5.5	0.6	1.7	0	0.009
	2			1		5		-5.8	0.9	1.7	0	0.006
CLMA, rad^{-1}	21			11		53		-0.005	0.2	0.3	0	0.049
	13			2		28		+0.075	0.6	1.7	0	0.017
	7			1		15		-0.040	0.9	1.7	0	0.012
	6			2		14		-0.031	1.1	1.7	0	0.010
	3			2		8		+0.029	1.3	1.8	0	0.009
	12			12		36		+0.017	0.2	0.3	0	0.027
	4			2		10		+0.101	0.6	1.7	0	0.009
	4			1		9		-0.011	0.9	1.7	0	0.006
CLMT	3			12		18		+0.008	0.2	0.3	20	0.049
	1			2		4		+0.012	0.6	1.7	20	0.017
	1			1		3		-0.023	0.9	1.7	12	0.012
	1			1		3		-0.021	1.1	1.7	12	0.010
	1			1		3		-0.067	1.3	1.8	19	0.009
	3			12		8		+0.020	0.2	0.3	12	0.027
	2			2		6		+0.001	0.6	1.7	12	0.009
	1			1		3		-0.022	0.9	1.7	15	0.006
RFP, rad^{-1}		7.1×10^{-4}			2.8×10^{-3}		4.2×10^{-3}	0.049	0.2	0.3		
		2.2×10^{-5}			1.7×10^{-4}		2.1×10^{-4}	0.017	0.6	1.7		
		8.3×10^{-6}			1.1×10^{-4}		1.3×10^{-4}	0.012	0.9	1.7		
		5.5×10^{-6}			9.0×10^{-5}		1.0×10^{-4}	0.010	1.1	1.7		
		4.5×10^{-6}			7.9×10^{-5}		8.8×10^{-5}	0.009	1.3	1.8		
		4.2×10^{-4}			1.7×10^{-3}		2.5×19^{-3}	0.027	0.2	0.3		
		1.2×10^{-5}			9.2×10^{-5}		1.2×10^{-4}	0.009	0.6	1.7		
		4.5×10^{-6}			6.0×10^{-5}		6.9×10^{-5}	0.006	0.9	1.7		

*Abernethy, R. B. et al. and Thompson, J. W. "Handbook Uncertainty in Gas Turbine Meas urements," AEDC-TR-73-5 (AD 755356), February 1973.

VB-16a (9-79)

APPENDIX II

SAMPLE OF TABULATED AND PLOTTED DATA

DATE COMPUTED 6-NV-79
TIME COMPUTED 15:27: 4
DATE RECORDED 2-OCT-79
TIME RECORDED 17:54:42
PROJECT NUMBER P41C-A9

PROPULSION WIND TUNNEL FACILITY
ARNOLD AIR FORCE STATION, TENNESSEE
SUPPORT INTERFERENCE STUDY-TRANSONIC PHASE

RUN	M	CONFIG	A	D	L	PHIM	PHIR	INERTIA
208	.8993	19	.3491	.6667	.6667	0.00	0.00	.40938

PLATF= 0. LP/D= .00 LS/D= 3.30 K= .0000

ALPHA	BETA	CLMO	CLMA	CLMT	REDX10-6	PT	TT	Q	V	P	RFP	GAMMA	THETA	PB1	PB2
-0.10	-0.00	-5.847	-0.0114	-0.0063	1.666	1266.3	557.2	424.2	965.5	5.20324	0.006416	86.9	0.968	0.8671	0.8682
-0.10	-0.00	-6.654	-0.0102	-0.0004	1.672	1270.3	557.2	425.9	966.2	5.21552	0.006411	88.6	0.960	0.8636	0.8645
3.70	0.00	-6.913	-0.0039	-0.0068	1.671	1269.2	557.1	426.0	967.1	5.20511	0.006393	87.8	0.969	0.8527	0.8540
7.49	0.00	-7.592	-0.0140	-0.0143	1.662	1268.8	557.1	424.7	964.7	5.21774	0.006418	79.4	0.979	0.8344	0.8368
11.29	0.00	-9.212	-0.0034	-0.0199	1.670	1269.8	557.0	424.6	963.9	5.22606	0.006406	82.2	0.978	0.8181	0.8208
11.30	0.00	-8.759	0.0074	-0.0198	1.671	1269.8	557.0	424.9	964.5	5.22248	0.006402	87.6	0.984	0.8184	0.8204
15.23	0.00	-8.692	-0.0433	-0.0225	1.673	1270.1	557.0	426.1	966.5	5.21196	0.006478	84.4	1.007	0.8004	0.8036
19.09	-0.00	-9.079	-0.0948	-0.0281	1.675	1271.9	557.0	426.5	966.1	5.22162	0.006588	90.8	0.975	0.7740	0.7780
19.07	-0.00	-9.043	-0.0931	-0.0283	1.663	1262.4	556.9	423.4	966.3	5.18106	0.006586	92.8	0.977	0.7777	0.7809
-0.10	-0.00	-5.435	-0.0161	-0.0004	1.666	1264.2	556.9	424.8	967.8	5.17882	0.006411	86.4	0.996	0.8693	0.8711

SAMPLE 1. TABULATED SUMMARY DATA

SYMBOL	CONFIG	LS/D	PHIB	M	REDX10^{-6}	RFP	RUNS
⊙	[illegible]	3.3	0	0.90	4.7	0.0064	208

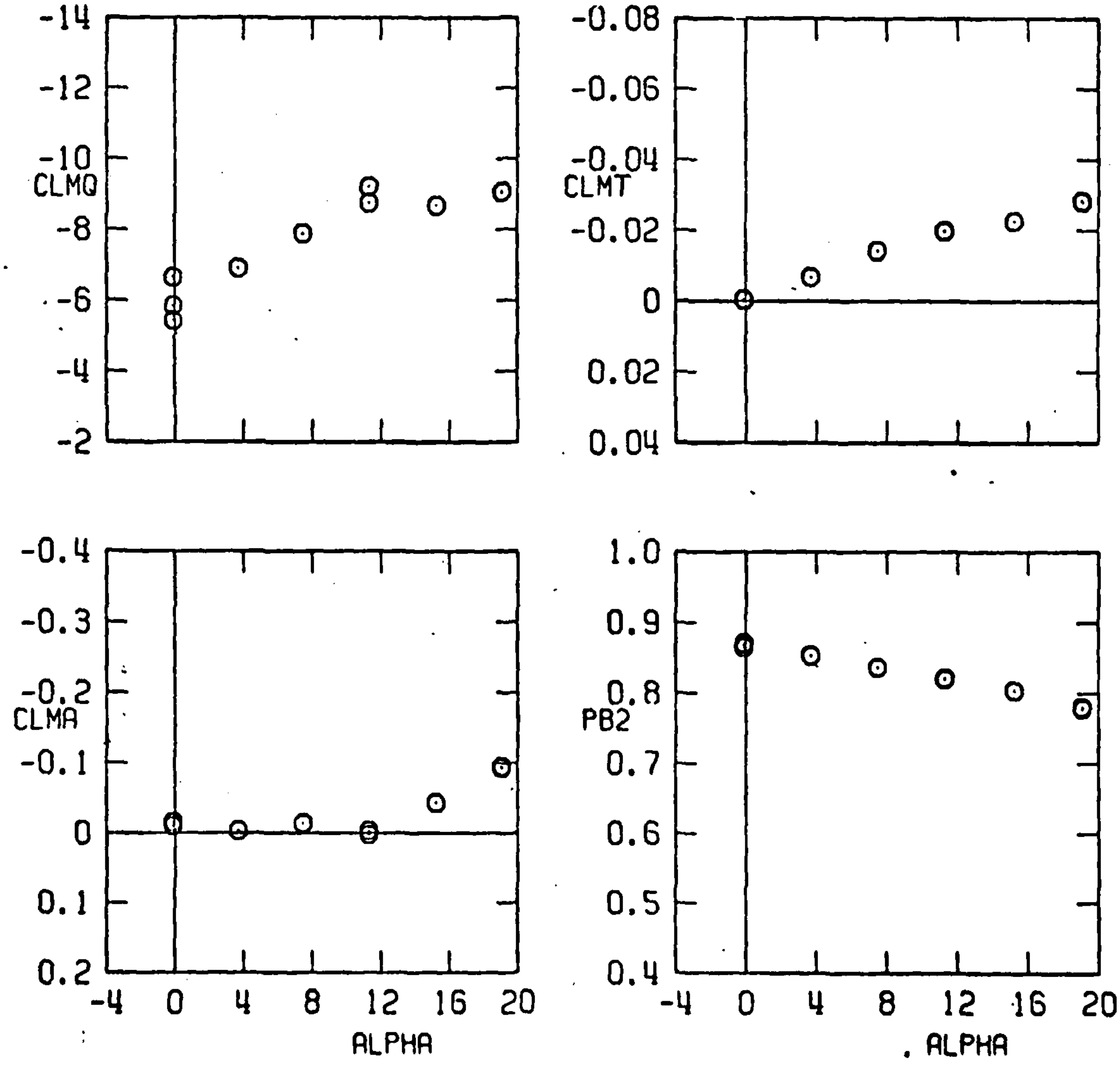

SAMPLE 2. PLOTTED DATA

DAT

ILM